

Supplemental Materials: A composite ansatz for the calculation of dynamical structure factor

Yupei Zhang,¹ Chongjie Mo,^{2,*} Ping Zhang,^{3,4} and Wei Kang^{4,†}

¹*HEDPS, Center for Applied Physics and Technology, and School of Physics, Peking University, Beijing 100871, China*

²*Beijing Computational Science Research Center, Beijing 100193, China*

³*Institute of Applied Physics and Computational Mathematics, Beijing 100088, China*

⁴*HEDPS, Center for Applied Physics and Technology, and College of Engineering, Peking University, Beijing 100871, China*

(Dated: December 18, 2023)

The supplemental materials contain four sections. In Sec. I, a collection of calculated dynamical structure factors (DSF) of lithium (Li) at different transferred momenta \mathbf{q} along [100], [110] and [111] directions are presented and compared with inelastic x-ray scattering (IXS) measurements. Three theoretical models, i.e., the TDDFT method with ALDA kernel (denoted as ALDA), the TDDFT with life-time correction method proposed by Weissker *et al.* [1] (denoted as ALDA+LT), and the new method that contains the contribution from both the TDDFT kernel and from the Green's function (denoted as ALDA+G), are used in the calculation. In Sec. II, a collection of calculated DSF of silicon (Si) at various transferred momenta and directions are presented and compared with available experiments. The theoretical methods used are the same as those in the calculation of Li. In Sec. III, quasi-particle properties, including the renormalization factor, the quasi-particle energy shift, the life-time broadening, of Li and Si are displayed with respect to corresponding Kohn-Sham eigen-energies. In Sec. IV, two transferred-momentum cases of DSF calculations for polycrystalline sodium (Na) are presented and compared with IXS measurements.

I. DSF OF LI AT DIFFERENT TRANSFERRED MOMENTA AND DIRECTIONS

In addition to the DSFs displayed in the main text, calculated DSF of Li at other transferred momenta and directions are shown in Fig. 1, Fig. 2 and Fig. 3. Fig. 1 displays DSF of Li along the [100] direction, where $|\mathbf{q}|$ varies from 0.28 bohr^{-1} to 1.40 bohr^{-1} . As shown in Fig. 1 (a) and (b), for $|\mathbf{q}| < q_c$, the plasmon peak can be well determined by the ALDA, ALDA+LT, and our ALDA+G method. It shows that the life-time broadening can be approximated as a constant broadening in these cases.

Fig. 1(c) and (d) display DSF of $|\mathbf{q}|$ between q_c and $2q_c$. The single plasmon peak of DSF now transforms into a

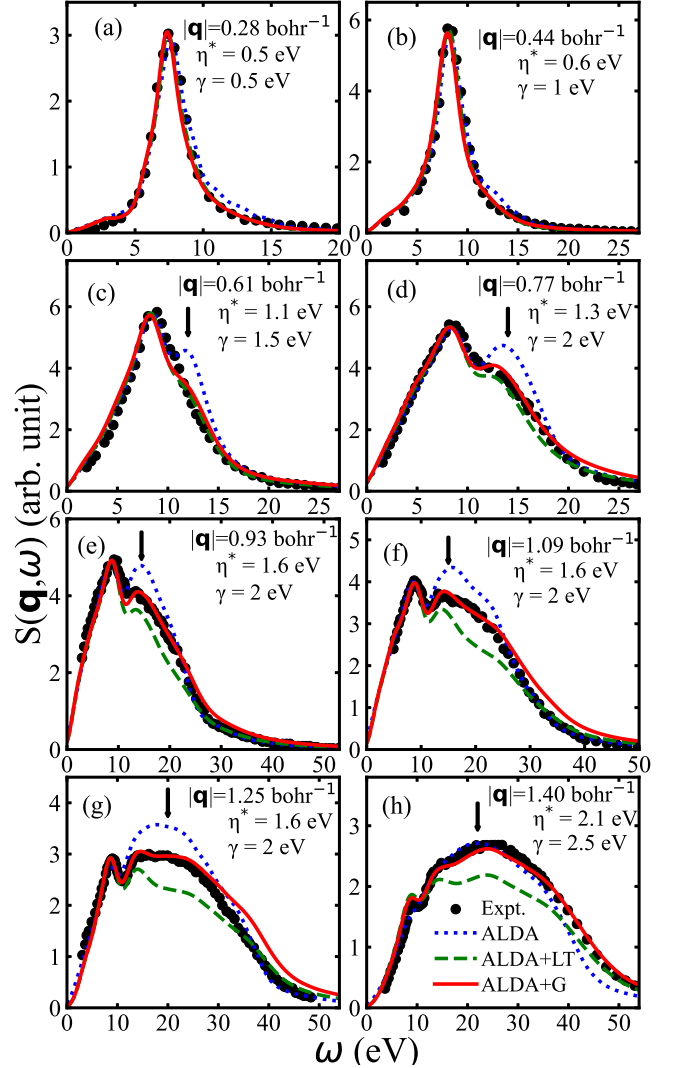


FIG. 1. Calculated DSF of Li together with IXS spectra measured by Schülke *et al.* [2] along the [100] direction. Solid scattering dots are IXS measurements, solid red curves are results calculated with the “ALDA+G” method, “ALDA+LT” results are displayed with dashed green curves, and dotted blue curves show the results of the “ALDA” method.

* cjmo@csrc.ac.cn

† weikang@pku.edu.cn

double-peak structure. The second peak in the spectrum

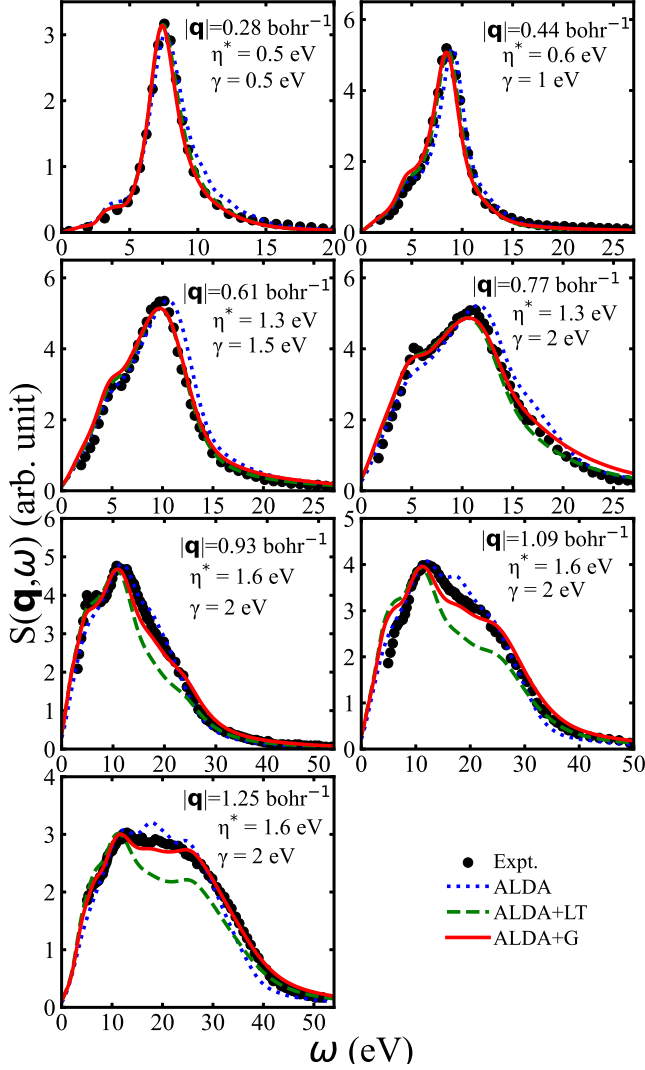


FIG. 2. Calculated DSF of Li for \mathbf{q} along [110] together with experimental measurements of Schülke *et al.* [2]

predicted by ALDA is higher than the experimental measurements, as highlighted by the arrows, indicating that the exchange-correlation kernel f_{xc} in ALDA is not sufficient to account for the spectrum for $|\mathbf{q}| > q_c$. Weissker *et al.* [1] realized that this deviation was caused by the lack of a proper broadening, and thus included the imaginary part of quasi-particle energy as the energy-dependent lifetime broadening, which turns out capturing the essential feature of DSF for $|\mathbf{q}| < 2q_c$, as displayed by the ALDA+LT results. This correction is naturally included in our new method as part of the Green's function. As displayed by the ALDA+G results in Fig. 1(c) and (d), both methods reproduce the experimental results well.

Fig. 1(e)-(h) displays the cases where the renormalization factor of the Green's function has to be included in the theory, through the rescaling coefficient Γ defined in the main text. The comparison between the ALDA+G and ALDA+LT results, of which the former includes the

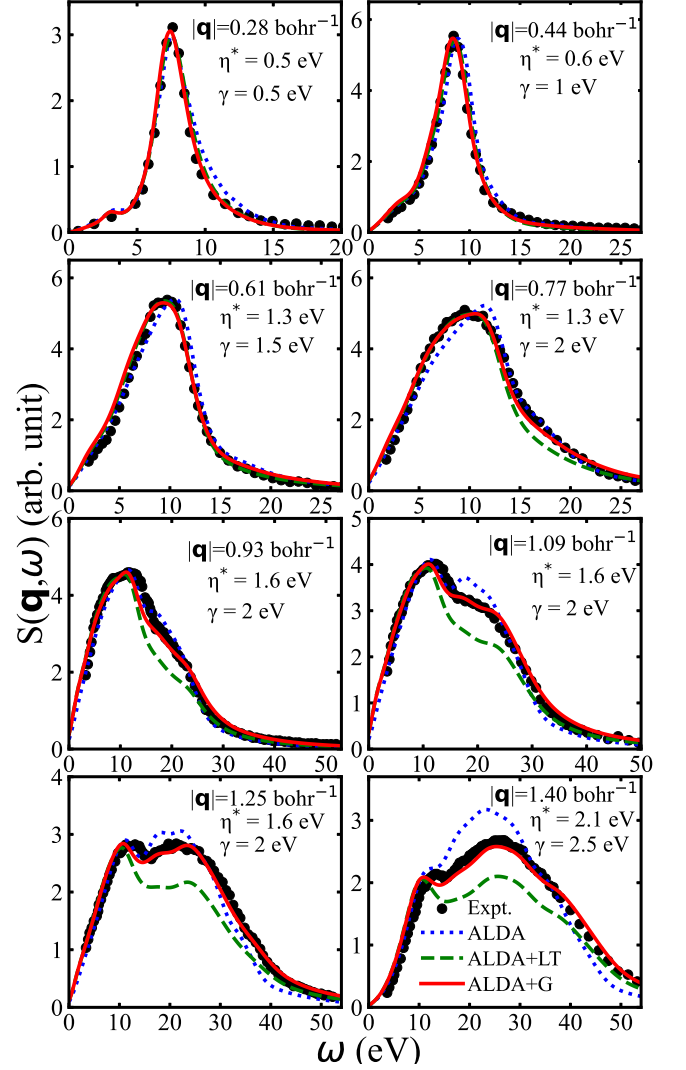


FIG. 3. Calculated DSF of Li for \mathbf{q} along [111] together with experiments of Schülke *et al.* [2]

contribution of the renormalization factor, and the latter does not, shows that the renormalization factor affords a necessary rescaling which lifts the strength of the spectra at high energy. Similar results along the [110] and [111] directions are shown in Fig. 2 and Fig. 3.

II. DSF OF SI AT VARIOUS TRANSFERRED MOMENTA AND DIRECTIONS

In this section, we present calculated DSF of bulk Si. Fig. 4 includes results along the [111] direction, Fig. 5 is results along the [100] direction, and Fig. 6 is for the [110] direction.

In the figures, the calculated results are compared with two independent experimental measurements from Schülke *et al.* in early 1990's [2, 4] and Weissker *et al.* [1, 3] in middle 2000's. It should be noticed that the ex-

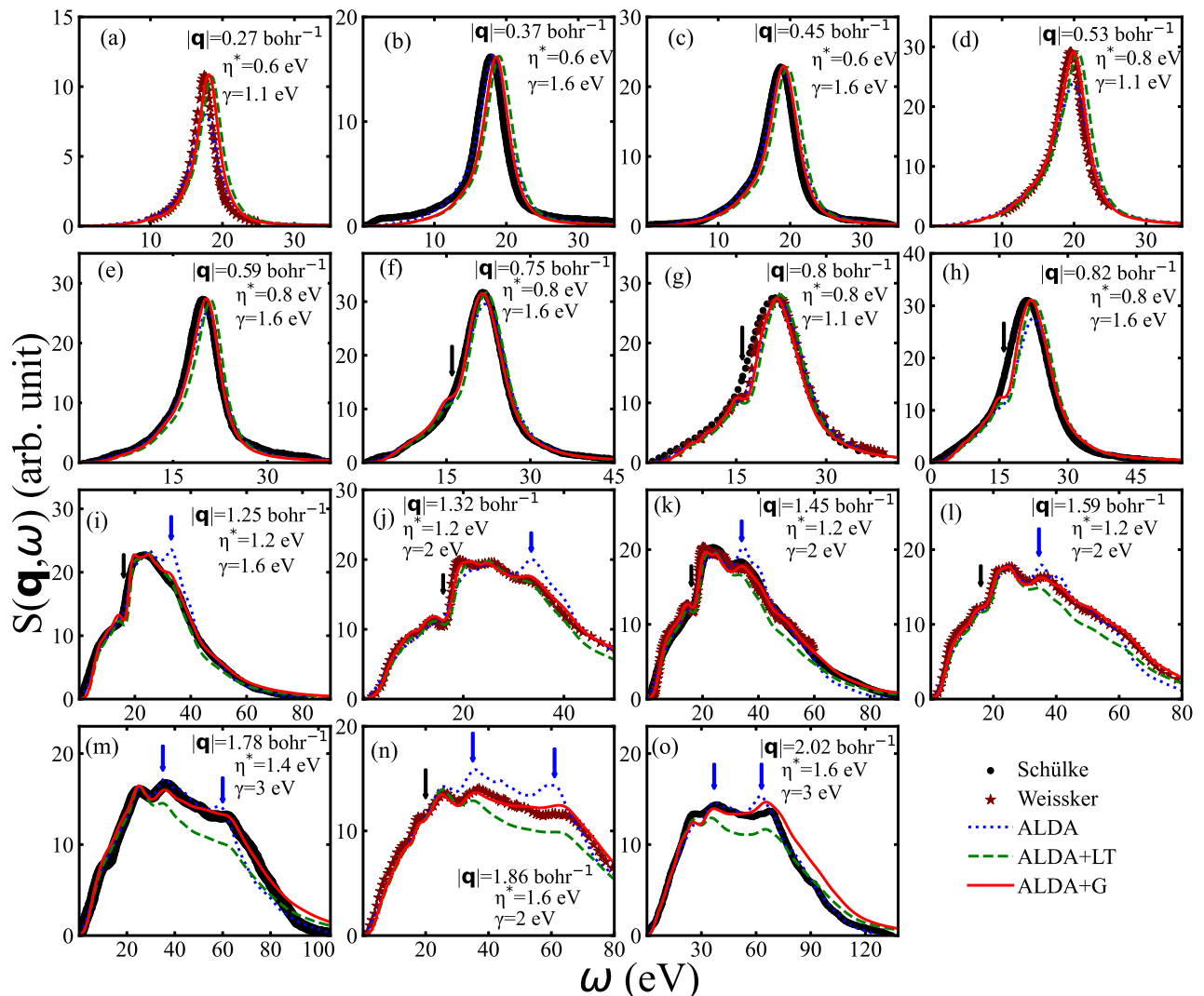


FIG. 4. Calculated DSF of Si together with IXS spectra measured by Schülke *et al.* [2] and Weissker *et al.* [1, 3] along the [111] direction. Solid scattering dots are IXS measurements, solid red curves are results of the “ALDA+G” method, “ALDA+LT” results are displayed with dashed green curves, and dotted blue curves show the results of the “ALDA” method.

periments of Schülke *et al.* were carried out with much less accuracy as revealed by Weissker *et al.* in much recent experiments. For example, as displayed in Fig. 4(g) and Fig. 5(a), there are prominent differences between these two measurements. Our calculated DSFs not only agree well with the recent measurements of Weissker *et al.* in overall feature of the spectra, they are also capable to reproduce the subtle fluctuating ripples in the experimental measurements, for example, as displayed in Fig. 4(g), (i)-(l), and (n), as well as Fig. 5(a),(g)-(j), where some subtle features are indicated by arrows.

III. QUASI-PARTICLE PROPERTIES OF LI AND SI

Fig. 7 displays quasi-particle properties of Li and Si, including the modulus of renormalization factor $|Z_j|$, the quasi-particle energy shift $\Delta^{QP} = \Re[\epsilon_j^{QP}] - \epsilon_j^{KS}$, and the life-time broadening $\tau^{-1}/2 = |\Im[\epsilon_j^{QP}]|$ of the j -th quasi-particle state, with respect to the corresponding Kohn-Sham eigen-energy ϵ_j^{KS} . They are original data used for the calculation of the rescaling coefficient Γ , the quasi-particle energy shift Δ , and the life-time broadening η of electron-hole pairs in Fig. 2 of the main text.

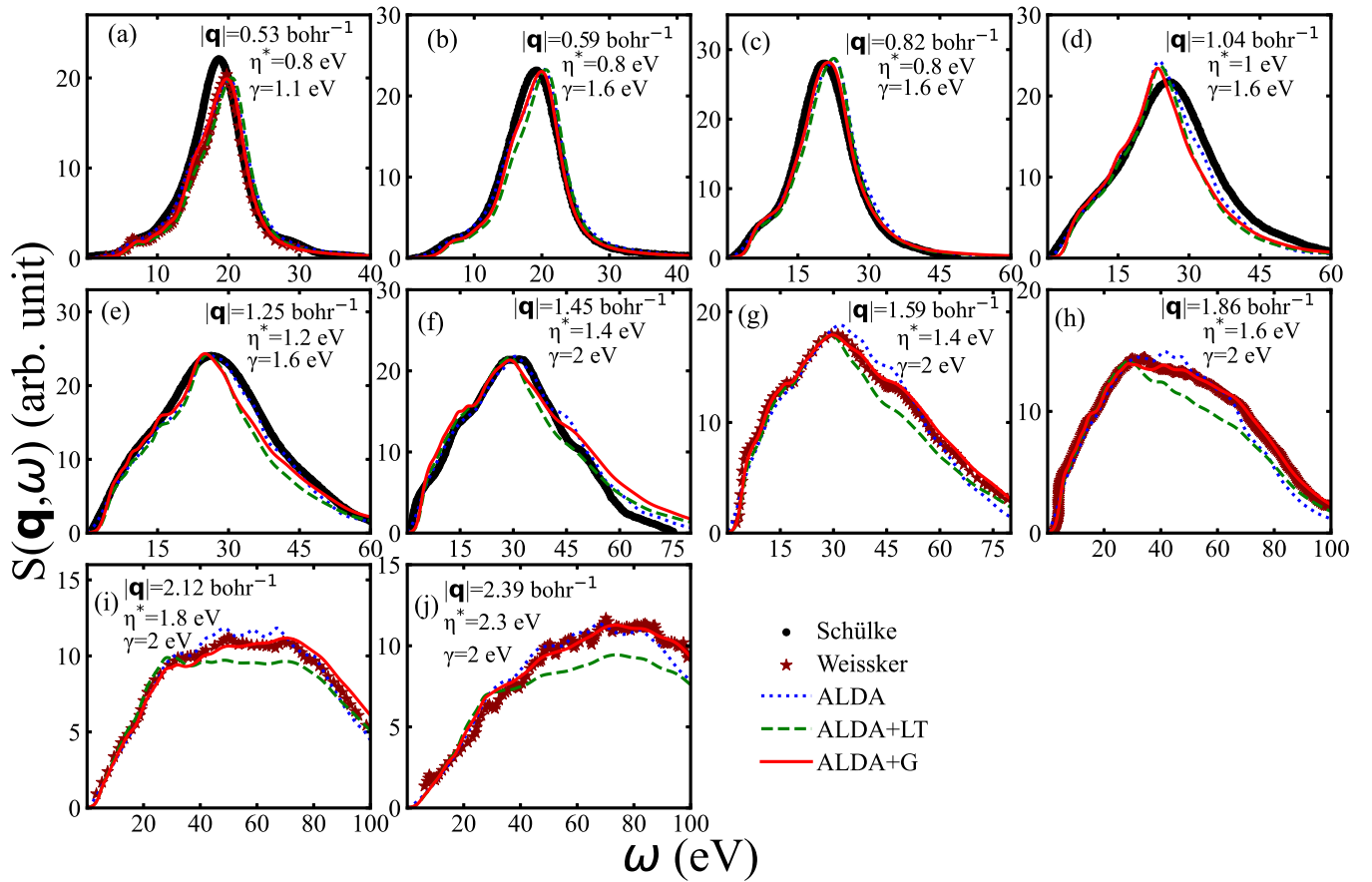


FIG. 5. Calculated DSF of Si for \mathbf{q} along [100] together with experimental measurements.

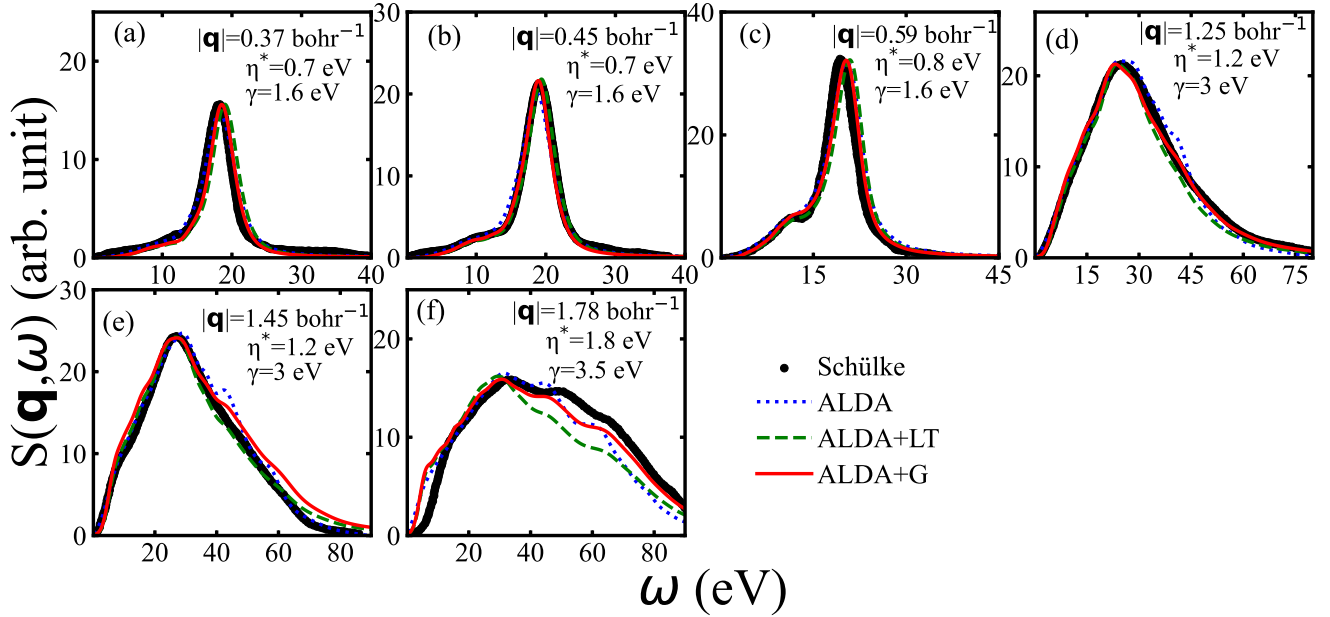


FIG. 6. Calculated DSF of Si for \mathbf{q} along [110] together with experimental measurements.

IV. DSF OF NA

Na, measured by Reining *et al* [5, 6] are the latest results.

Fig. 8 displays the DSFs of polycrystalline Na with $|\mathbf{q}| = 0.27$ and 1.16 bohr^{-1} . The experimental data for

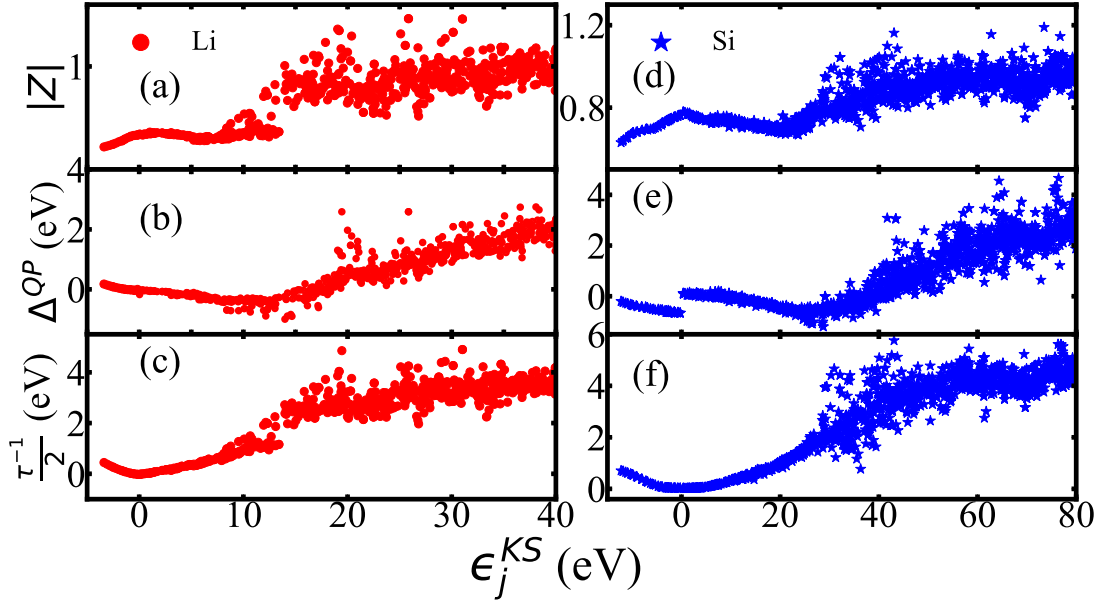


FIG. 7. Quasi-particle properties of Li and Si. (a) Modulus of renormalization factor $|Z|$; (b) Quasi-particle energy shift Δ^{QP} ; and (c) life-time broadening $\tau^{-1}/2$ calculated using the GW method. All properties are plotted with respect to the corresponding Kohn-Sham eigen-energies.

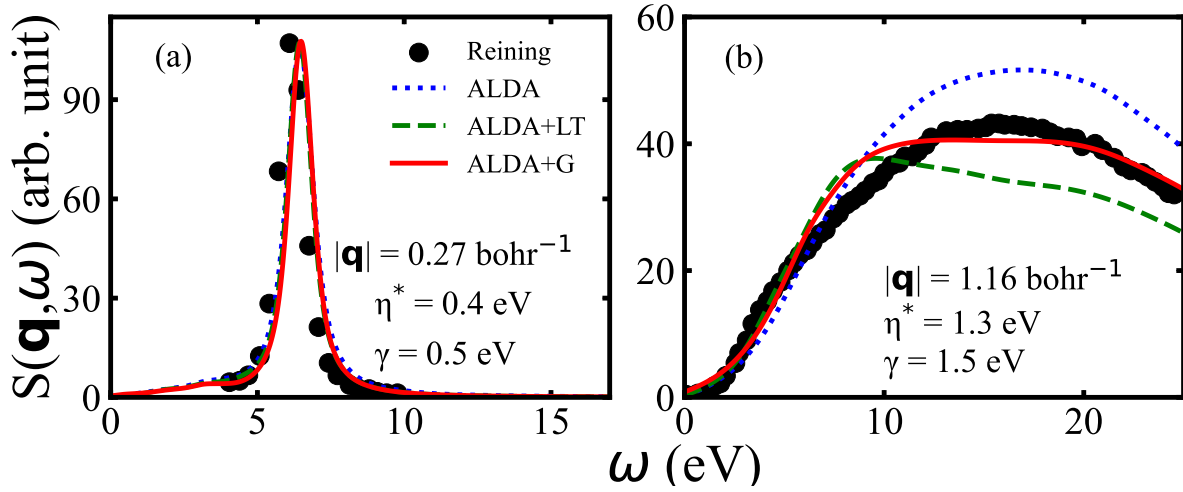


FIG. 8. Calculated DSFs of Na together with experiments of Reining *et al* [5, 6]. Solid scattering dots are IXS measurements, solid red curves are results of the “ALDA+G” method, “ALDA+LT” results are displayed with dashed green curves, and dotted blue curves show the results of the “ALDA” method.

As shown in Fig. 8 (a), for $|\mathbf{q}| = 0.27 \text{ bohr}^{-1}$, the DSF calculated by ALDA+G is consistent with ALDA, and ALDA+LT methods which is in good agreement with the measurement. For a large transferred momentum, the differences between those three methods emerge. As shown in Fig. 8 (b), the intensity of DSF at a high energy

predicted by ALDA is much larger than that of measurement, while ALDA+LT underestimates it. By introducing the effect of renormalization factor, the ALDA+G method significantly enhances the intensity of DSF at a high energy compared with ALDA+LT, resulting in a better agreement with the measurement.

[1] H.-C. Weissker, J. Serrano, S. Huotari, F. Bruneval, F. Sottile, G. Monaco, M. Krisch, V. Olevano, and L. Rein-

ing, Phys. Rev. Lett. **97**, 237602 (2006).

- [2] W. Schülke, J. R. Schmitz, H. Schulte-Schrepping, and A. Kaprolat, *Phys. Rev. B* **52**, 11721 (1995).
- [3] H.-C. Weissker, J. Serrano, S. Huotari, E. Luppi, M. Cazzaniga, F. Bruneval, F. Sottile, G. Monaco, V. Olevano, and L. Reining, *Phys. Rev. B* **81**, 085104 (2010).
- [4] K. Sturm, W. Schülke, and J. R. Schmitz, *Phys. Rev. Lett.* **68**, 228 (1992).
- [5] M. Cazzaniga, H.-C. Weissker, S. Huotari, T. Pylkkänen, P. Salvestrini, G. Monaco, G. Onida, and L. Reining, *Phys. Rev. B* **84**, 075109 (2011).
- [6] S. Huotari, M. Cazzaniga, H.-C. Weissker, T. Pylkkänen, H. Müller, L. Reining, G. Onida, and G. Monaco, *Phys. Rev. B* **84**, 075108 (2011).